

Supporting Information

Photochemistry using Host-Guest Charge Transfer Paradigm: DMABN as a Dynamical Probe of Ground and Excited States

Rahul Gera and Jyotishman Dasgupta^{†*}

[†]Department of Chemical Sciences, Tata Institute of Fundamental Research, Mumbai 400005, India.

*Email: dasgupta@tifr.res.in

Contents:

1. Materials and Methods	S2- S3
2. The synthesis of Pd₆L₄ cage	S4
3. The synthesis of inclusion complex DMABN ⊂ Cage	S4
4. Structural Information from NMR: Through Space proton-proton distances	S5-S10
5. Time-evolution of the broad Visible excited state absorption signal	S11
6. Kinetics of excited state absorption signal in Visible	S12
7. Time-evolution of the broad NIR excited state absorption signal	S13
8. Kinetics of excited state absorption signal in NIR	S14

Supplementary Figures:

S1 : 1D- NOE difference spectrum for DMABN ⊂ cage obtained by saturating proton Hb of DMABN	S6
S2 : 1D- NOE difference spectrum for DMABN ⊂ cage obtained by saturating proton Me of DMABN	S7
S3 : 1D- NOE difference spectrum for DMABN ⊂ cage obtained by saturating proton Me of DMABN	S8
S4 : 1D- NOE difference spectrum for DMABN ⊂ cage obtained by saturating proton Me of DMABN	S9
S5 : Time-evolution of the broad NIR excited state absorption signal in DMABN ⊂ Cage after excitation with $\lambda_{\text{pump}} = 490$ nm	S11
S6 : Kinetics of excited state absorption signal for DMABN ⊂ Cage at 545 nm after excitation with $\lambda_{\text{pump}} = 490$ nm.	S12
S7 : Time-evolution of the broad NIR excited state absorption signal in DMABN ⊂ Cage after excitation with $\lambda_{\text{pump}} = 490$ nm.	S13
S8 : Kinetics of excited state absorption signal for DMABN ⊂ Cage at 880 nm after excitation with $\lambda_{\text{pump}} = 490$ nm.	S14
S9 : Kinetics of excited state absorption feature at 952 nm for DMABN ⊂ cage after excitation with 490 nm pump pulse	S15

Supplementary Table:

ST1: Calculated distances between ¹ H close in space using NOE difference spectroscopy	S10
--	-----

1. Materials and Methods:

Solvents and reagents were purchased from TCI Co., Ltd., S.D. Fine Chemicals and Sigma-Aldrich Co. D₂O was acquired from Sigma-Aldrich Co, Inc. and used as supplied for the reactions and NMR measurements.

NMR Measurements:

¹H and other 2D NMR spectra were recorded on Bruker (500 MHz, and 700 MHz) and Varian (600 MHz) spectrometer.

Steady State Absorption Measurements:

Absorption measurements were carried out in SPECORD 205 spectrophotometer. All the measurements were collected from 200-800 nm.

Transient Measurements:

Time-resolved transient measurements were carried out using an amplified laser source. 400 mW output from a mode-locked Ti:sapphire oscillator, MICRA-5, operating at 80 MHz repetition rate with a bandwidth of ~ 100 nm was amplified using a Coherent Legend Elite amplifier to provide a pulsed output of 4 W with spectral bandwidth of 65 nm and temporal bandwidth of 30 fs at 1 KHz repetition rate. The 4 mJ/pulse amplified output was split into two beams of equal power with help of a beam splitter. One portion is used for generation of a tunable output from an optical parametric amplifier (Coherent OPeraASolo). Other portion is used for generation of probe pulse, which is a white light continuum (~ 400 -1600 nm) generated using a 2 mm thick sapphire crystal. The optical parametric amplifier was used to generate 490 nm pump pulse which was attenuated to get an output of ~ 200-400 nJ per pulse that reaches the sample. The probe and the actinic pump pulses were focused, and overlapped temporally and spatially on the sample within a flow cuvette with 1 mm thickness. After passing through the sample, the probe photons were detected using a multichannel detector (Ultrafast Systems, Sarasota, Fl). Delay between pump and probe pulses were controlled using a motorized Newport translation stage that has a qudra-pass mirror assembly. 1 mm flow-cell with a 0.5 mm thick window was used for measurements. The flow rate was adjusted to replenish fresh sample and prevent photobleaching. NMR measurements were done pre- and post to the transient measurements to check the integrity of the host-guest complex. We detected no change of the samples after measurement. The samples in H₂O were prepared along with the samples in D₂O under identical conditions, and the measurements were performed under same settings to have a good comparison of the two datasets. The temporal instrument response is a Gaussian, with a FWHM of ~ 100 fs. The $t = 0$ between pump and probe pulses was assigned using cross-correlation and comparison to solvent response but, it was allowed to vary freely while fitting the kinetics. Fitting of

kinetics was done using a multi-exponential model convoluted with the IRF using home written codes in IGOR 5 Pro. Singular value decomposition (SVD) of the transient data was carried out by Surface Explorer[®] software from Ultrafast Systems.

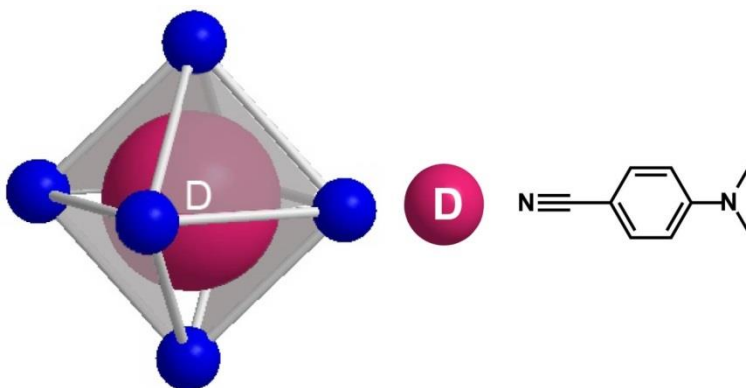
2. Synthesis of the cationic (Pd_6L_4) cage:

Cage preparation can be found M. Fujita *et al. Nature* 1995, 378, 469 and R. Gera *et al. J. Am. Chem. Soc.* 2014, 136, 15909. Protons of ethylenediamine are in the aliphatic region at δ 2.90 ppm. Reported values for proton H_α is δ 8.98 ppm as it is near to N ligated to Pd^{2+} thus downfield in comparison to H_β (δ 8.48 ppm).

^1H – NMR of cage 1 (600MHz, D_2O , 298 K): δ 9.00 (d, pyridine- α), 8.51 (d, pyridine- β), 2.90 (s, Hc).

3. Synthesis of the inclusion complex $\text{DMABN} \subset \text{cage}$:

DMABN \subset cage inclusion complex was synthesized using the synthetic route reported by R. Gera *et al. J. Am. Chem. Soc.* **2014**, 136, 15909. Water insoluble DMABN solid (~ 19 mg) was stirred with a 5 ml solution of 2.5 mM cage 1 in D_2O for 1 h at room temperature. The colorless cage solution changes to orange. The solution was filtered through a 0.45 μ filter to remove the residual solid. Residual solid was removed by filtration using 0.45 micron filter. The host-guest complex in H_2O was synthesized simultaneously under identical conditions to avoid any ambiguity. The complex formation was confirmed by ^1H NMR and stability was tested before and after each spectroscopic measurement. ^1H –NMR of $\text{DMABN} \subset \text{Cage}$ (500MHz, D_2O , 298 K): δ 9.27 (d, pyridine- α , Cage), 8.65 (d, pyridine- β , Cage), δ 5.24 (d, H_a , DMABN), δ 4.94 (d, H_b , DMABN), δ 2.94 (s, H_c , Cage), δ 1.40 (s, Me, DMABN); [Inset DMABN free in solution, (600 MHz, CDCl_3 , 298 K): δ 7.46 (d, H_a , DMABN), δ 6.64 (d, H_b , DMABN), δ 3.03 (s, Me, DMABN)].



4. Structural Information from NMR: Through Space proton-proton distances

These measurements were carried out on 700 MHz BRUKER NMR spectrometer at room temperature.

A proton pairs (I and S) give rise to NOE intensity when present close in space ($\sim 4 - 5 \text{ \AA}$), for a given mixing time. NOE intensity is proportional to the I-S cross relaxation rate (σ_{IS})

η_{IS} = intensity of the NOE between I and S, τ_m is experimental mixing time.

$$\eta_{IS} = \sigma_{IS}\tau_m$$

Cross relaxation rate is proportional to the internuclear distances (r_{IS}^{-6}) described by

$$\sigma_{IS} = kr_{IS}^{-6}$$

Here,

$$k = \left(\frac{\mu_0}{4\pi}\right) \frac{\hbar^2\gamma^4}{10} \left(\frac{6\tau_c}{1 + 4\omega^2\tau_c^2} - \tau_c\right)$$

μ_0, γ , and ω is equivalent for a given experiment.

Selective saturation of a spin in a given transient 1D-NOESY spectrum would reflect in change of intensities of protons correlated to it in spatial proximity. Difference spectrum of an off-resonance spectrum with an on resonance saturation spectrum, will provide the information about protons correlated to each other in space. Assuming k is also constant, and then the ratio of the intensities of a pair of NOE signals η_{IS} : η_{I2S} within that spectrum can be proportional to their ratio of internuclear distances and this ratio will be independent of mixing time.

$$\frac{\eta_{I1S}}{\eta_{I2S}} = \frac{r_{I1S}^{-6}}{r_{I2S}^{-6}} \quad \dots (1)$$

Distances were calculated using the nondispersive features in NOE difference spectrums.

Distance calculation between Hb and Me - difference NOE spectrum of DMABN \subset Cage

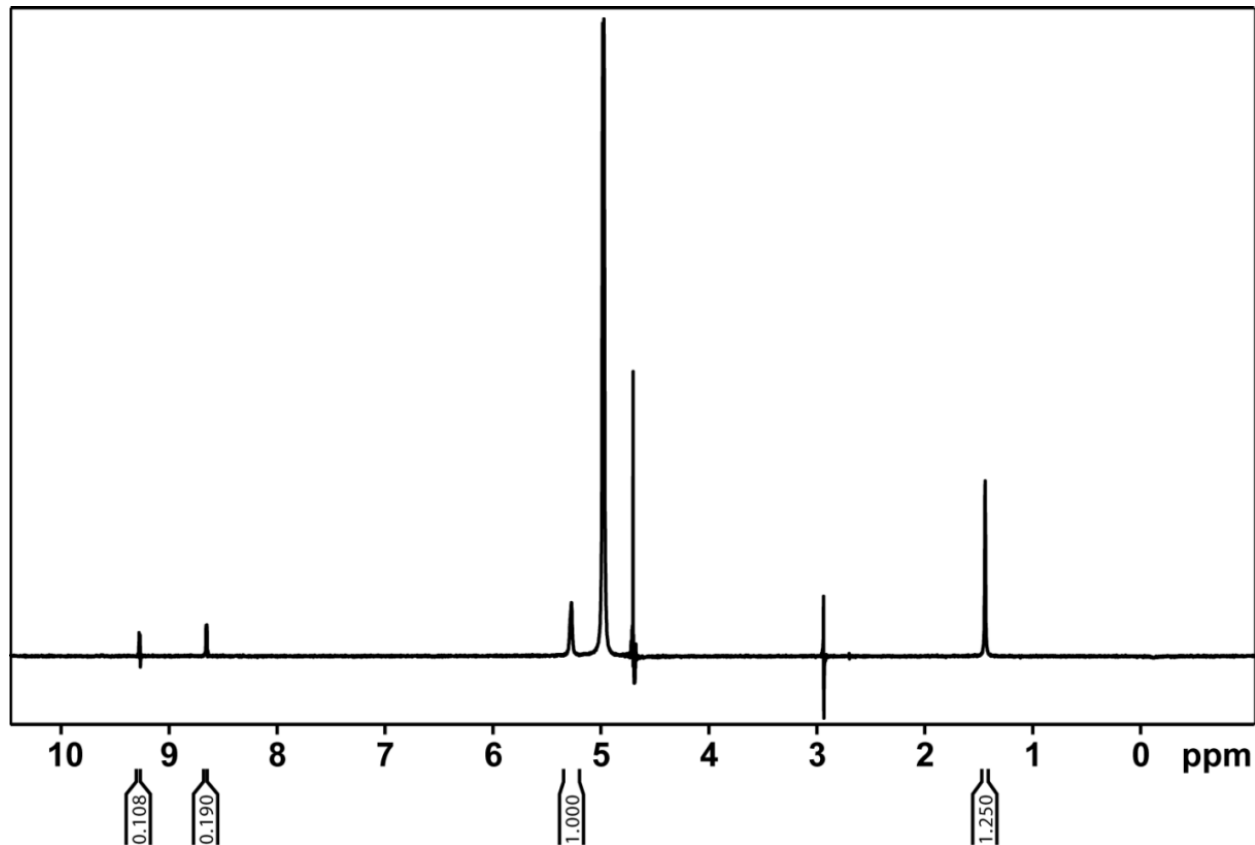
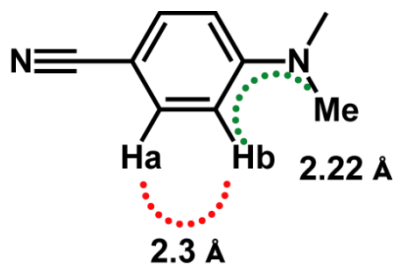


Figure S1. 1D- NOE difference spectrum for DMABN \subset cage obtained by saturating proton Hb of DMABN

Here, I = Hb, 1S = Ha, 2S = Me, $\eta_{HbHa} = 1$, $\eta_{HbMe} = 1.25$, $r_{HbHa} = 2.3 \text{ \AA}$

$$\frac{\eta_{I1S}}{\eta_{I2S}} = \frac{r_{I1S}^{-6}}{r_{I2S}^{-6}} \Rightarrow \frac{\eta_{HbHa}}{\eta_{HbMe}} = \frac{r_{HbHa}^{-6}}{r_{HbMe}^{-6}} = \frac{1}{1.25} = \frac{2.3^{-6}}{r_{HbMe}^{-6}} \Rightarrow r_{HbMe} = 2.22 \text{ \AA}$$



Distance calculation between Ha and Me - difference NOE spectrum of DMABN \subset Cage

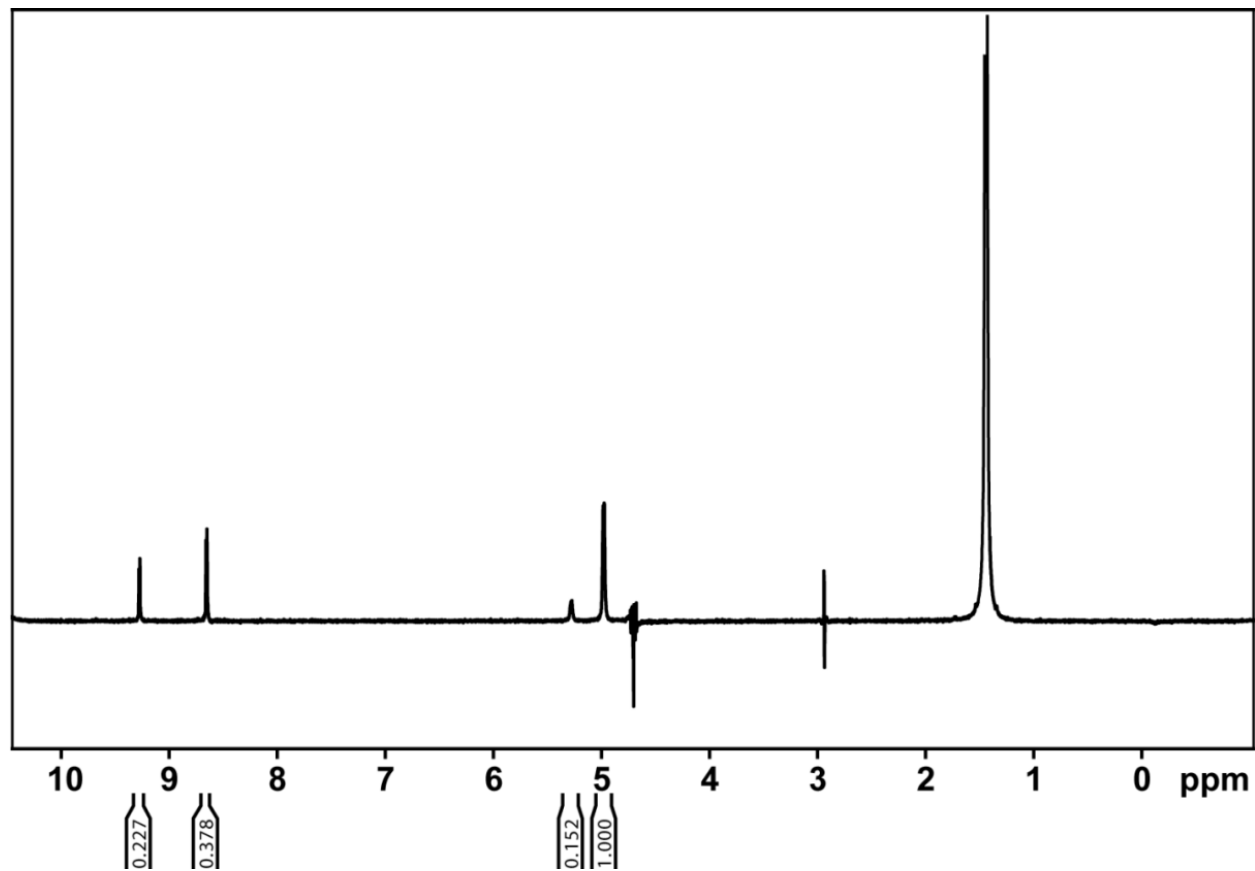
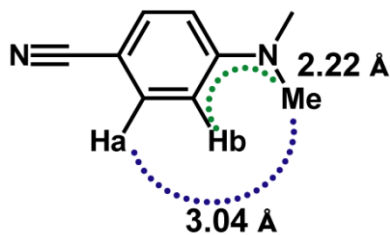


Figure S2. 1D- NOE difference spectrum for DMABN \subset cage obtained by saturating proton Me of DMABN

$$I = \text{Me}, 1S = \text{Hb}, 2S = \text{Ha}, \eta_{\text{MeHb}} = 1, \eta_{\text{MeHa}} = 0.152, r_{\text{MeHb}} = 2.22 \text{ \AA}$$

$$\frac{\eta_{\text{MeHb}}}{\eta_{\text{MeHa}}} = \frac{r_{\text{MeHb}}^{-6}}{r_{\text{MeHa}}^{-6}} = \frac{1}{0.152} = \frac{2.22^{-6}}{r_{\text{MeHa}}^{-6}} \Rightarrow r_{\text{MeHa}} = 3.04 \text{ \AA}$$



Distance calculation between H β and Me - difference NOE spectrum of DMABN \subset Cage

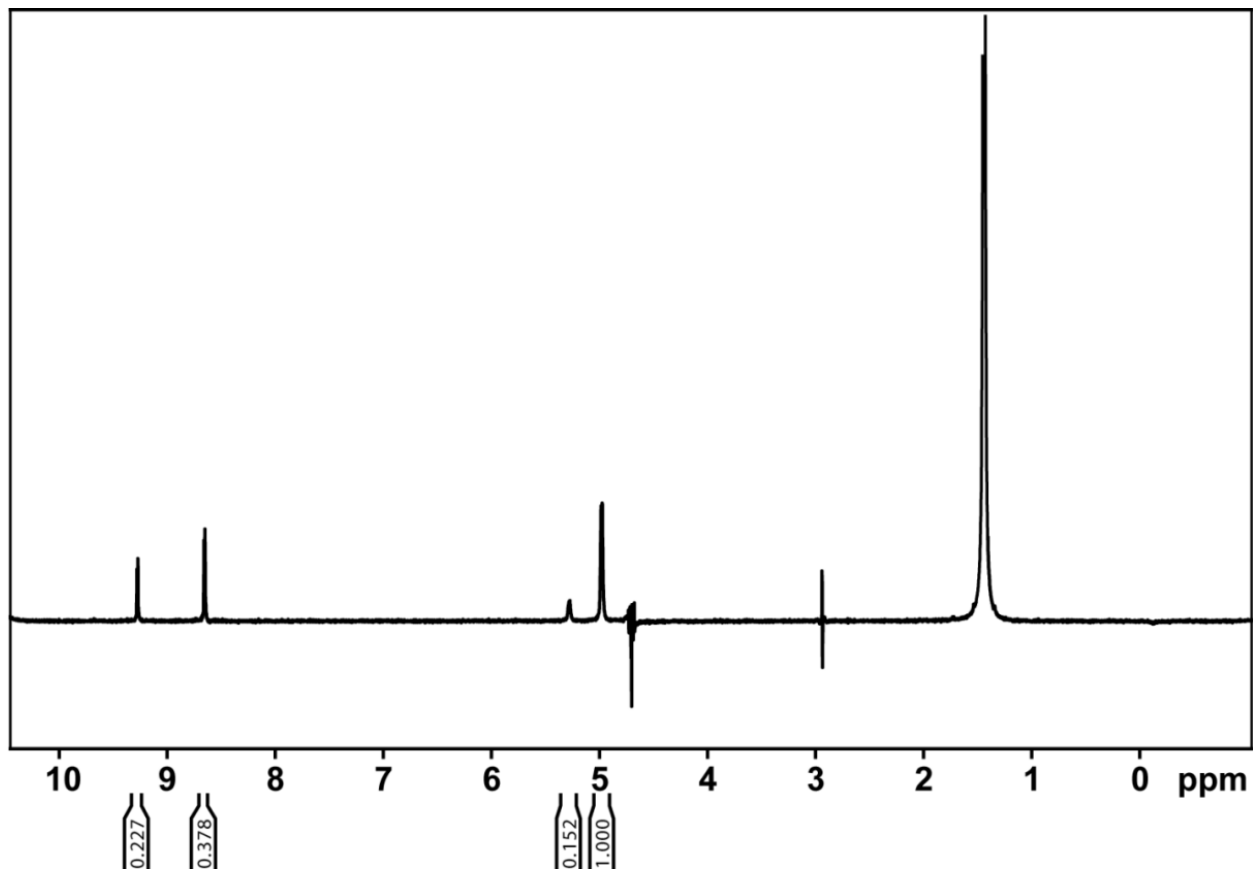
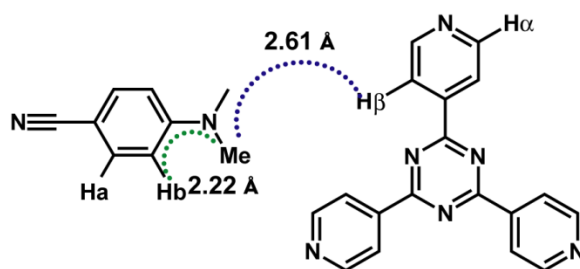


Figure S3. 1D- NOE difference spectrum for DMABN \subset cage obtained by saturating proton Me of DMABN

$$I = \text{Me}, 1S = \text{H}\beta, 2S = \text{H}\alpha, \eta_{\text{MeH}\beta} = 1, \eta_{\text{MeH}\alpha} = 0.378, r_{\text{MeH}\beta} = 2.22 \text{ \AA}$$

$$\frac{\eta_{\text{MeH}\beta}}{\eta_{\text{MeH}\alpha}} = \frac{r_{\text{MeH}\alpha}^{-6}}{r_{\text{MeH}\beta}^{-6}} = \frac{1}{0.378} = \frac{2.22^{-6}}{r_{\text{MeH}\alpha}^{-6}}$$

$$r_{\text{MeH}\alpha} = 2.61 \text{ \AA}$$



Distance calculation between H α and Me - difference NOE spectrum of DMABN \subset Cage

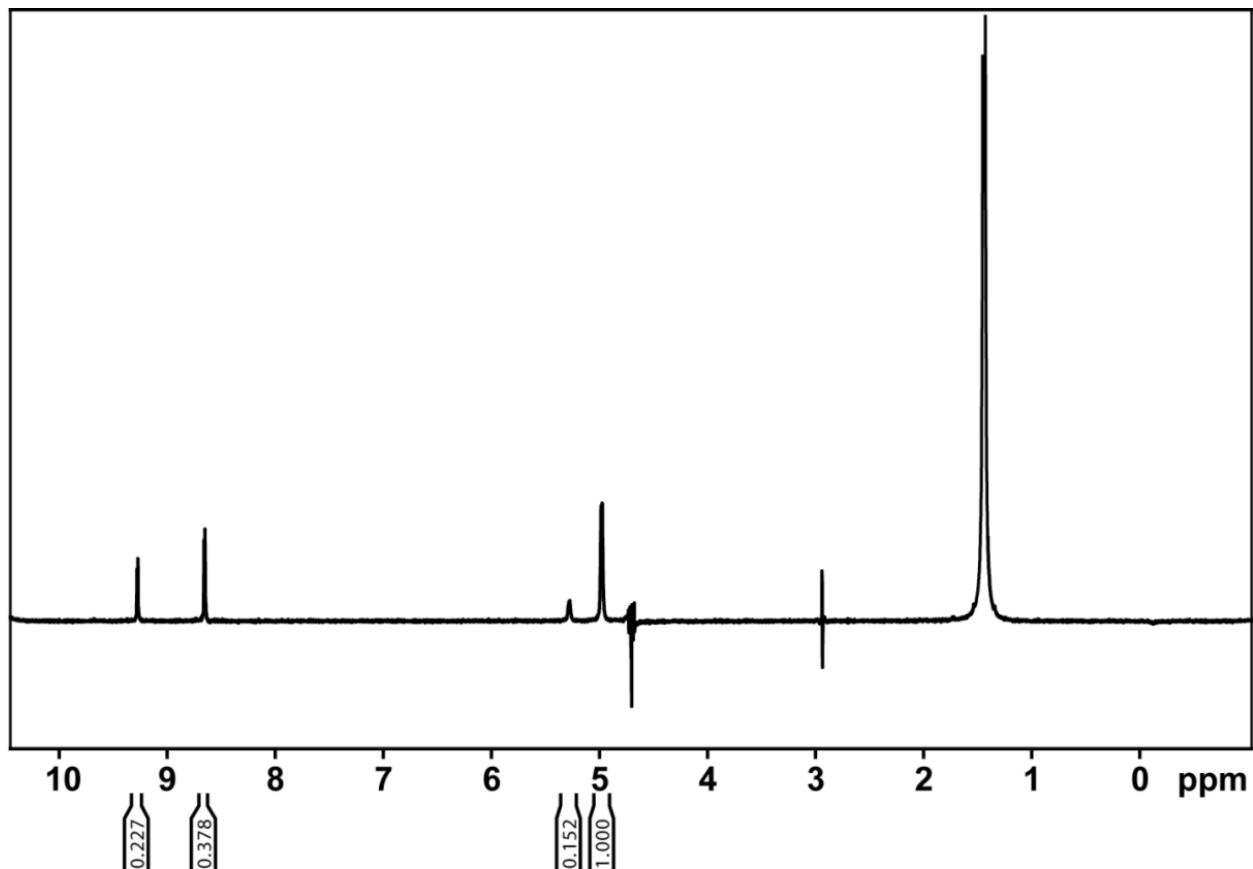
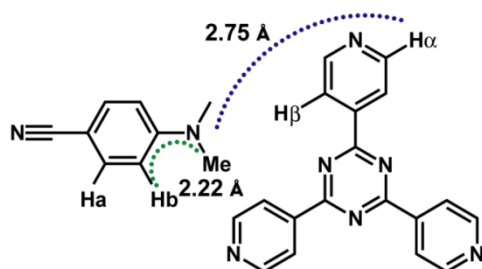


Figure S4. 1D- NOE difference spectrum for DMABN \subset cage obtained by saturating proton Me of DMABN

$$I = \text{Me}, 1S = \text{H}\beta, 2S = \text{H}\alpha, \eta_{\text{MeH}\beta} = 1, \eta_{\text{MeH}\alpha} = 0.378, r_{\text{MeH}\beta} = 2.22 \text{ \AA}$$

$$\frac{\eta_{\text{MeH}\beta}}{\eta_{\text{MeH}\alpha}} = \frac{r_{\text{MeH}\beta}^{-6}}{r_{\text{MeH}\alpha}^{-6}} = \frac{1}{0.227} = \frac{2.22^{-6}}{r_{\text{MeH}\alpha}^{-6}}$$

$$r_{\text{MeH}\alpha} = 2.75 \text{ \AA}$$



Pair of protons	Spatial distances (Å)
Hb (DMABN) - Me (DMABN)	2.20
Ha (DMABN) - Me (DMABN)	3.04
Me (DMABN) - H α (Cage)	2.75
Me (DMABN) - H β (Cage)	2.61

Table ST1. Calculated distances between ^1H close in space using NOE difference spectroscopy

5. Time-evolution of the broad Visible excited state absorption signal

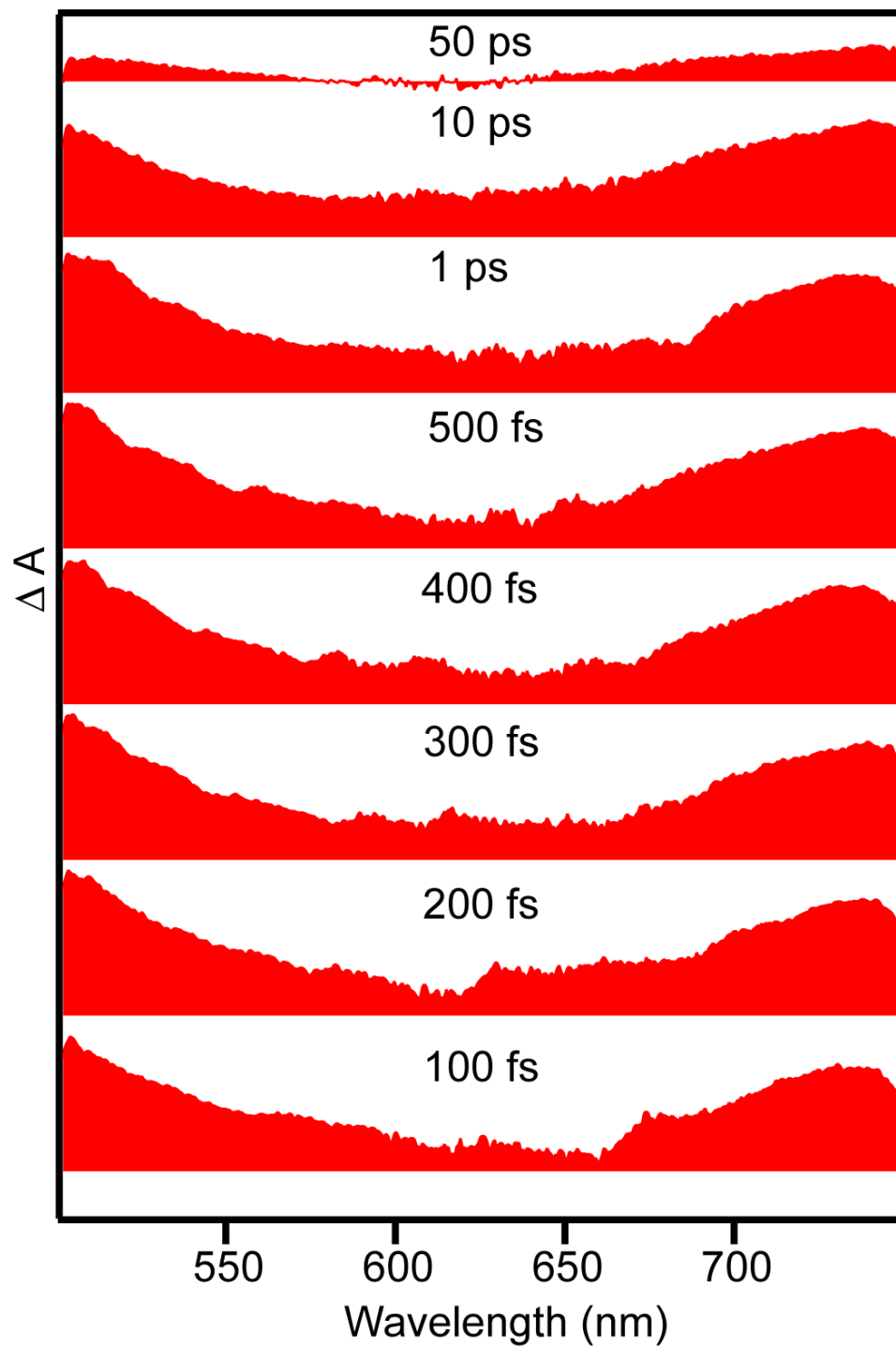


Figure S5. Time-evolution of the broad NIR excited state absorption signal in DMABN \subset Cage after excitation with $\lambda_{\text{pump}} = 490$ nm.

6. Kinetics of excited state absorption signal in Visible

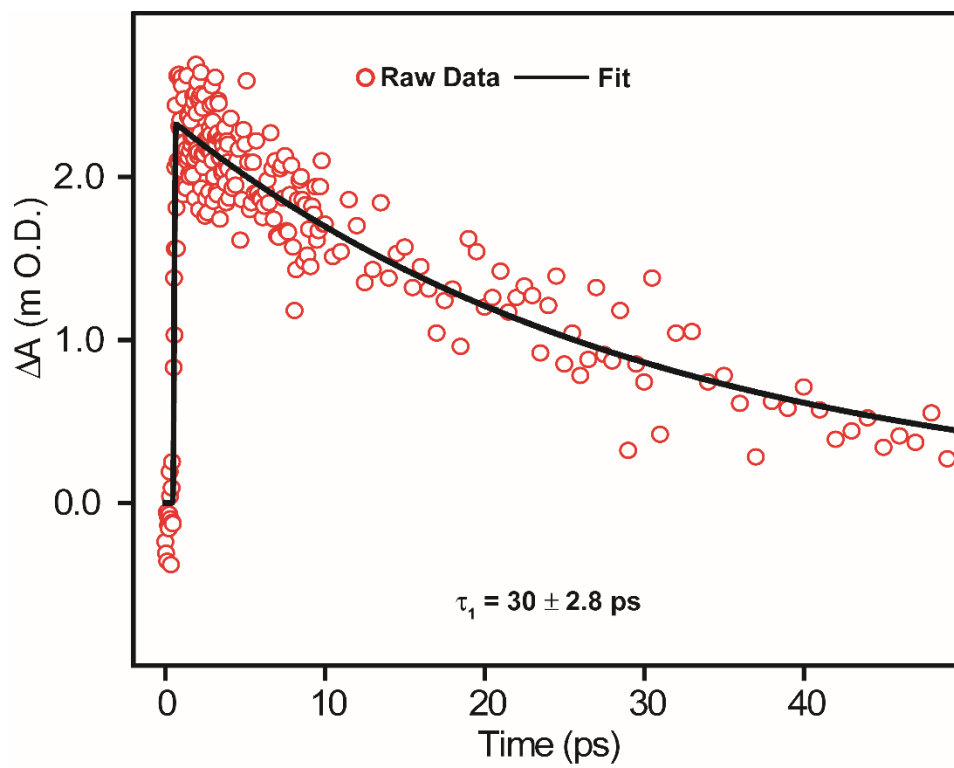


Figure S6. Kinetics of excited state absorption signal for DMABN \subset Cage at 545 nm after excitation with $\lambda_{\text{pump}} = 490$ nm.

7. Time-evolution of the broad NIR excited state absorption signal

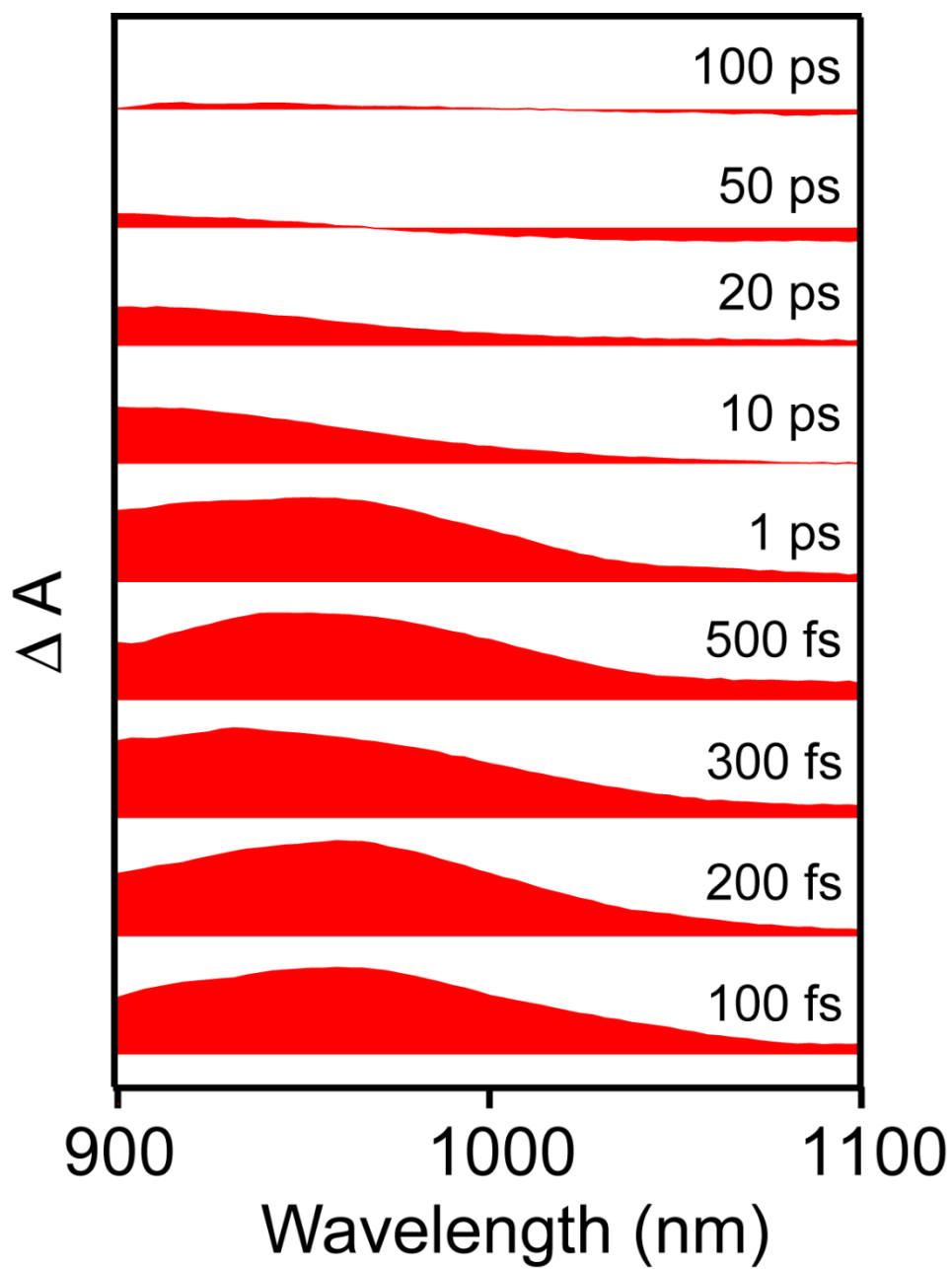


Figure S7. Time-evolution of the broad NIR excited state absorption signal in DMABN \subset Cage after excitation with $\lambda_{\text{pump}} = 490$ nm.

8. Kinetics of excited state absorption signal in NIR

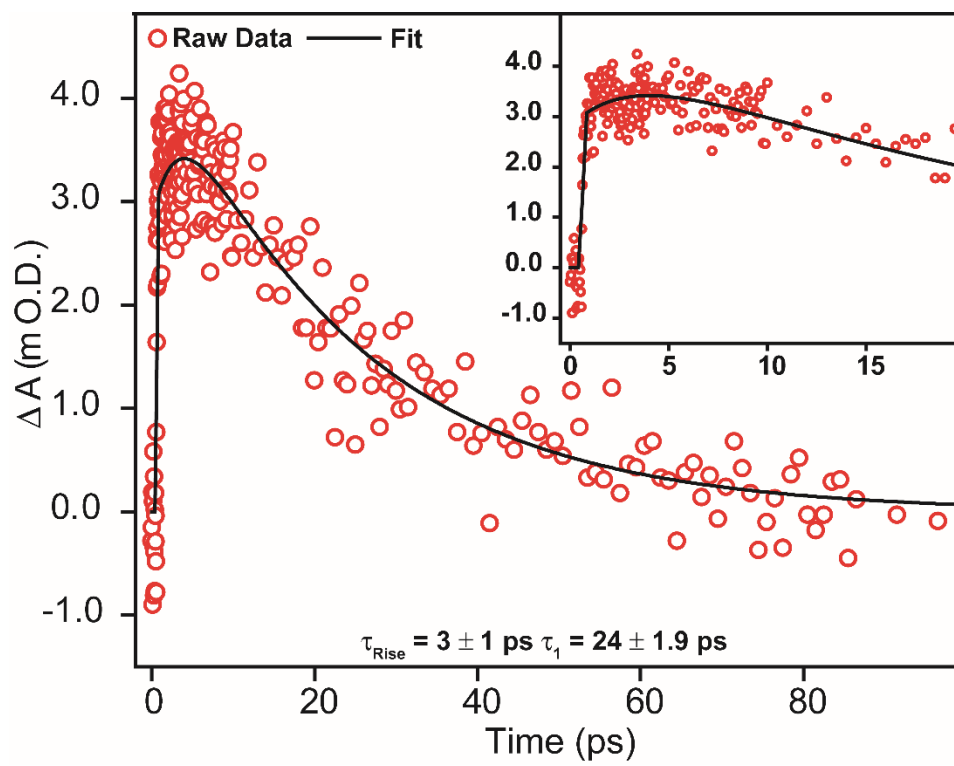


Figure S8. Kinetics of excited state absorption signal for DMABN \subset Cage at 880 nm after excitation with $\lambda_{\text{pump}} = 490$ nm.

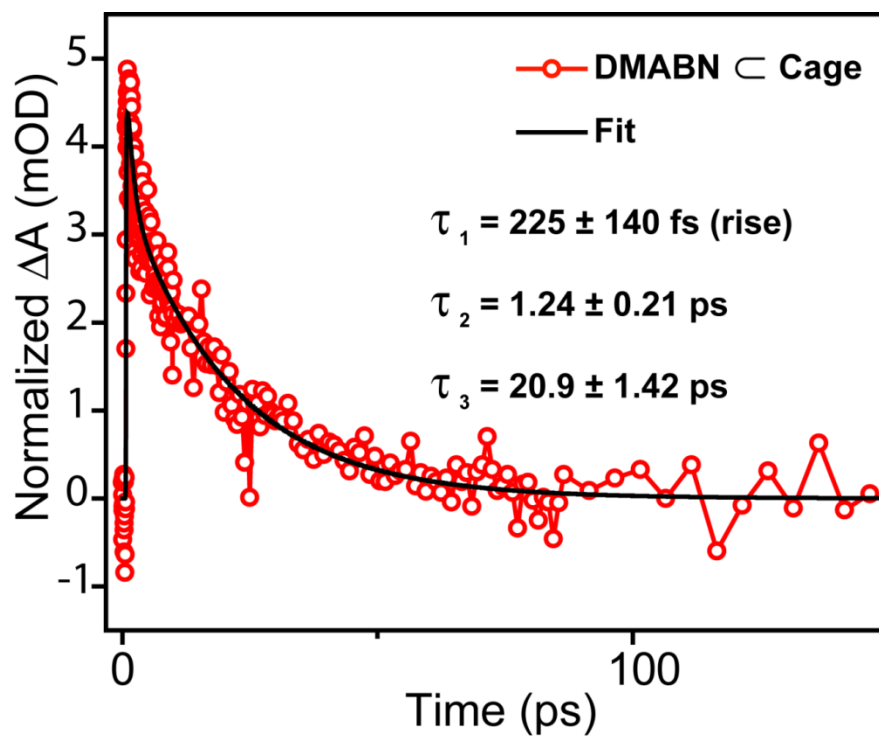
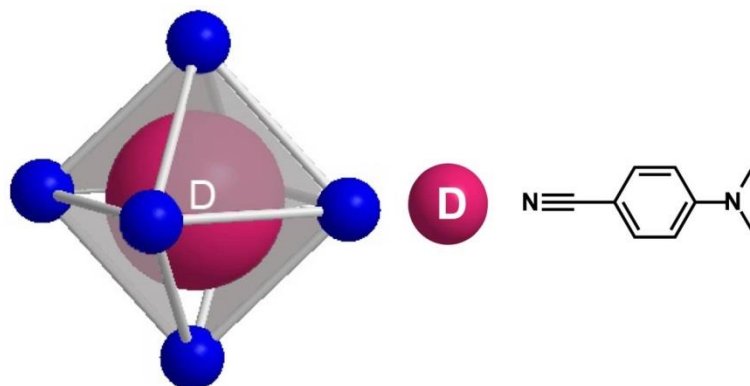


Figure S9. Kinetics of excited state absorption feature at 952 nm for DMABN \subset cage after excitation with 490 nm pump pulse. This data is also included the published manuscript R. Gera *et al. J. Am. Chem. Soc.* 2014, 136, 15909.